International Immunology, Vol. 29, No. 12, pp. 551–566
doi:10.1093/intimm/dxx063
Advance Access publication 15 November 2017

FEATURED ARTICLE

Lysosome biogenesis regulated by the amino-acid transporter SLC15A4 is critical for functional integrity of mast cells

Toshihiko Kobayashi[1], Hidemitsu Tsutsui[1], Shiho Shimabukuro-Demoto[1], Reiko Yoshida-Sugitani[1], Hitomi Karyu[1], Kaori Furuyama-Tanaka[1], Daisuke Ohshima[1], Norihiro Kato[2], Tadashi Okamura[3] and **Noriko Toyama-Sorimachi[1]**

[1]Department of Molecular Immunology and Inflammation,
[2]Department of Gene Diagnostics and Therapeutics and
[3]Department of Infectious Disease, Research Institute, National Center for Global Health and Medicine, 1-21-1 Toyama, Shinjuku-ku, Tokyo 162-8655, Japan

Correspondence to: N. Toyama-Sorimachi; E-mail: nsorima@ri.ncgm.go.jp

Received 2 October 2017, *editorial decision* 6 November 2017; *accepted* 14 November 2017

Abstract

Mast cells possess specialized lysosomes, so-called secretory granules, which play a key role not only in allergic responses but also in various immune disorders. The molecular mechanisms that control secretory-granule formation are not fully understood. Solute carrier family member 15A4 (SLC15A4) is a lysosome-resident amino-acid/oligopeptide transporter that is preferentially expressed in hematopoietic lineage cells. Here, we demonstrated that SLC15A4 is required for mast-cell secretory-granule homeostasis, and limits mast-cell functions and inflammatory responses by controlling the mTORC1–TFEB signaling axis. In mouse *Slc15a4*$^{-/-}$ mast cells, diminished mTORC1 activity increased the expression and nuclear translocation of TFEB, a transcription factor, which caused secretory granules to degranulate more potently. This alteration of TFEB function in mast cells strongly affected the FcεRI-mediated responses and IL-33-triggered inflammatory responses both *in vitro* and *in vivo*. Our results reveal a close relationship between SLC15A4 and secretory-granule biogenesis that is critical for the functional integrity of mast cells.

Keywords: amino-acid transporter, IL-33, inflammation, secretory granules, TFEB

Introduction

Solute carrier family (SLC) member 15A4 is a lysosome-resident, proton-coupled histidine/oligopeptide transporter that has 12 membrane-spanning regions (1). SLC15A4 is preferentially expressed in immune cells, including dendritic cells and B cells (2, 3), and transports certain amino acids and oligopeptides—particularly histidine and the NOD1 ligand Tri-DAP—to the cytosol, along with a proton from the inside of the late endosome/lysosome (2, 4). SLC15A4 is critical for the TLR7- and TLR9-mediated production of type I interferon (IFN-I), for which SLC15A4's transporter activity is required to optimize pH and other conditions in the late endosomes/lysosomes for lysosome-dependent signaling events (2, 5–7). These intracellular TLR-signaling compartments are thought to differ from traditional lysosomes, which are specialized for catabolic processes, and are instead characterized as lysosome-related organelles (LROs) (8). In these compartments, SLC15A4 also plays a key role in IFNAR downstream signaling by regulating mTORC1's activity, which is required to establish the IRF7–IFN-I regulatory circuit (6). In SLC15A4-deficient mice, a decrease in IFN-I ameliorates lupus-like diseases and autoantibody production (6). Thus, the SLC15A4-mediated regulation of these signaling compartments is an integral part of innate immune responses and could significantly influence the pathogenesis of autoimmune diseases.

Lysosomes have long been regarded as waste bags containing an acidic interior for degrading intra- and extracellular materials (9). However, recent research has established that lysosomes are advanced organelles that are central in regulating membrane repair, macroautophagy, cell death, cholesterol homeostasis or other aspects of cellular homeostasis (9, 10). Immune cells utilize lysosomes not only for degradation, but also as a secretory pathway, for recycling and for signal transduction (11, 12). These LROs include heterogeneous vesicles such as cytotoxic granules in CD8$^+$

T cells and NK cells, platelet-dense granules and neutrophil azurophilic granules (8, 13). Maturing phagosomes in phagocytes such as dendritic cells, macrophages and neutrophils can also be considered inducible LROs (8), in which nucleic acid-sensing TLRs transmit signals to elicit innate immune responses. Although the molecular mechanisms of the biogenesis and maintenance of lysosomes and LROs are not fully understood, a clue emerged from the identification of transcription factor EB (TFEB), a master transcriptional regulator of lysosomal biogenesis and autophagy (12, 14–16). TFEB controls genes in the coordinated lysosomal expression and regulation (CLEAR) network, which coordinates and regulates a panel of genes involved in lysosome biogenesis and autophagy (16). TFEB's transcriptional activity is controlled downstream of the mTORC1 pathway (17, 18), which plays pivotal roles in cell growth and metabolism by sensing nutritional conditions. TFEB is phosphorylated by mTORC1 at the lysosomal surface, and the phosphorylated TFEB is retained outside the nucleus by associating with 14-3-3 proteins (18). Environmental cues such as starvation and lysosomal stress prompt the dephosphorylation of TFEB and its subsequent dissociation from the 14-3-3 proteins, leading to TFEB's nuclear translocation and decreased mTORC1 activity (15, 18). Forced TFEB expression and its consequent translocation to the nucleus alters lysosomal conditions, including the levels of lysosomal enzymes, lysosomal catabolic activity and lysosome exocytosis (16, 19). Thus, the TFEB-mediated regulation of lysosomes, including their biogenesis and functional adaptation, strongly affects a wide range of cellular activities. However, it is not clear whether TFEB is involved in cell-type-specific LRO functions or in disease pathogeneses *in vivo*.

Mast cells have well-developed LROs, also called secretory granules (20). These heterogeneous granules contain histamine and a panel of proteases and other inflammatory mediators, and their stored components and membrane proteins are not distributed uniformly (21). The molecular mechanisms that control secretory-granule formation are not fully understood. A deficiency of mast-cell granule components such as histamine and serglycin, a major proteoglycan found in the granules, results in poorly formed secretory granules (22, 23), indicating that some components of mast-cell secretory granules are important for granule formation.

Mast cells secrete granule contents in response to stimuli such as FcεRI cross-linking and G protein-coupled receptor-stimulating agents, and play key roles in the pathogenesis of anaphylaxis, asthma and allergy (24, 25). Mast cells also secrete *de novo*-synthesized cytokines such as IL-6 and IL-13 in response to infectious stimuli via TLRs, and modulate inflammation and acquired immune responses (26, 27). Mast cells secrete these cytokines when stimulated by growth factors and cytokines. The cytokine IL-33, which belongs to the IL-1 superfamily and is released from cells with damage-induced necrosis (28), is an important regulator of mast-cell functions in allergic inflammation (29–31). IL-33 binds the receptors ST2L and sST2; the former is a transmembrane form that can transmit signals, and the latter is a soluble form that is considered a decoy receptor (28). IL-33 acts on mast cells and other immune cells, including innate lymphoid cell 2 (ILC2) and NK cells, to regulate IL-13 production, leading to airway eosinophilia (32–34). Although mast cells' roles depend largely on their secretory functions, their secretion is phasic. Preformed secretory-granule components such as histamine, proteases and serotonin are secreted immediately by degranulation, and this early-phase response regulates the initial events in an inflammatory response, including type I hypersensitivity (35). In the later phase, mast cells secrete *de novo*-synthesized cytokines and mediators (late-phase response) (35). Thus, the biogenesis, maturation, and membrane trafficking of secretory granules and the process of secretion in mast cells appear to be tightly and coordinately regulated by multiple mechanisms, which remain largely unresolved.

Since mast cells express significant amounts of SLC15A4, which is important in lysosome-dependent and probably LRO-dependent cellular events, we examined whether SLC15A4 has a role in mast cells and in mast-cell-dependent pathogenic conditions. We here showed that SLC15A4 is required for regulating the pre-synthesized granule components and the secretory function in mast cells. We also showed that SLC15A4 is important for secreting *de novo*-synthesized cytokines downstream of the IL-33 receptor ST2L. The loss of SLC15A4 augmented the expression of CLEAR-network genes in mast cells by altering the mTORC1–TFEB signaling pathway, which appears to be involved in LRO homeostasis and LRO-dependent cytokine secretion in mast cells. Our results revealed a novel and unexpected functional linkage between the amino-acid transporter SLC15A4 and mast-cell LRO functions, which are important in mast-cell-mediated allergic inflammation.

Methods

Mice, cell lines and reagents

Slc15a4-deficient mice were generated as previously described (2). All animal experiments were approved by the Animal Care and Use Committee of the National Center for Global Health and Medicine (NCGM) Research Institute, and were conducted in accordance with institutional procedures. The P815 mouse mastocytoma line was purchased (American Type Culture Collection, VA, USA). The RBL-2H3 rat basophilic leukemia cell line and the anti-TNP mouse IgE (IGELb4) were kind gifts from H. Karasuyama (Tokyo Dental and Medical University). TNP-conjugated BSA (LGC Biosearch Technologies, CA, USA), *E. coli* LPS and 4-methylumbelliferyl-*N*-acetyl-β-glucosaminide (4-MUAG) (Sigma, MO, USA), histamine (Wako Pure Chemical Industries, Osaka, Japan), recombinant mouse IL-3 and mouse SCF (Peprotech, NJ, USA) and recombinant mouse IL-33 (R&D Systems, MN, USA) were purchased.

Mast-cell preparation

Bone marrow-derived mast cells (BMMCs) were prepared as follows: bone marrow cells taken from the femur or tibia of wild-type (WT) or *Slc15a4*$^{-/-}$ mice were cultured with IL-3 for 6–8 weeks, and the purity of the BMMCs was routinely confirmed by flow cytometry and staining with anti-FcεRIα (MAR-1) and anti-c-kit (2B8) mAbs. Peritoneal mast cells were enriched by following procedure: peritoneal cells were stained with PE-conjugated anti-FcεRIα (MAR-1) and FITC-conjugated anti-c-kit (2B8) mAbs, and double-positive cells were sorted on a FACSAria II (BD Biosciences, CA, USA).

Degranulation assay and cytokine quantification

To measure degranulation upon FcεRI ligation, BMMCs from WT or *Slc15a4*$^{-/-}$ mice were incubated overnight with anti-TNP IgE (clone IGELb4) in medium containing IL-3. Cells were washed twice with prewarmed Tyrode's buffer (10 mM HEPES pH 7.4, 130 mM NaCl, 5 mM KCl, 1 mM $MgCl_2$, 1.4 mM $CaCl_2$, 5.6 mM D-glucose and 0.1% BSA) and stimulated with TNP_4-BSA for 15 min or for the indicated periods in Tyrode's buffer. The supernatant was incubated with 4-MUAG (final concentration 0.5 mM) for 15 min at 37°C, and the reaction was stopped with Stop solution (2 M Na_2CO_3, 1.1 M glycine). Fluorescence (ex; 365 nm, em; 450 nm) was measured on a microplate reader (VarioScan Flash, Thermo Fisher, MA, USA). The degranulation rate was calculated by dividing the β-hexosaminidase (β-Hex) activity in the culture supernatant by the total cellular β-Hex activity, which was obtained from the supernatant of cells lysed with Tyrode's buffer containing 0.5% Triton-X 100. Cytokine levels in BMMC culture supernatants were measured with the Mouse ELISA Max Kit (BioLegend, CA, USA, for IL-6), or the Ready-Set-Go ELISA Kit (Thermo Fisher, for TNFα or IL-13).

Systemic anaphylaxis model

For IgE-mediated passive systemic anaphylaxis, mice were injected intravenously (i.v.) with 10 μg anti-TNP IgE (IGELb4) and challenged 24 h later with 400 μg of i.v. TNP_4-BSA. The rectal temperature of the mice was monitored over 60 min using a digital thermometer (Shibaura Electronics). To measure serum histamine levels, mice were sacrificed 90 s after the TNP_4-BSA challenge, and the sera were immediately isolated from blood obtained by cardiac puncture. For histamine-induced anaphylaxis, WT or *Slc15a4*$^{-/-}$ mice were given 5 mg histamine i.v., and the rectal temperature was monitored for 60 min. Histamine and serotonin levels in the mast-cell culture or sera were determined by a competitive enzyme immunoassay (EIA) (Bertin Pharma, France for histamine, and R&D Systems for serotonin).

IL-33-induced airway inflammation model

WT or *Slc15a4*$^{-/-}$ mice were sensitized with 25 ng of mouse IL-33 (R&D Systems) in combination with 100 μg OVA administered intraperitoneally (i.p.) on day 0 (d0), boosted on d7 and challenged intratracheally with 100 μg OVA from d17 to d19 (3 consecutive days). Bronchioalveolar lavage or peripheral blood was collected for flow cytometric analysis or measurement of antigen-specific antibody production, respectively, at d20. OVA-specific antibody production was measured as described below.

Measurement of immunoglobulins and antibody responses in vivo

Serum IgE levels in mouse sera were measured using a Mouse IgE ELISA Kit (BD Biosciences). To measure antigen-specific antibody levels, ELISA plates (Sumitomo Bakelite, Tokyo, Japan) were coated with 10 μg ml^{-1} OVA and OVA-specific antibodies were detected by HRP-conjugated isotype-specific antibodies (SouthernBiotech, AL, USA).

Flow cytometry

Single-cell suspensions were prepared from the peritoneal lavage, the spleen or the bone marrow of mice, and the cells were stained with the indicated mAbs and analyzed by flow cytometry using a BD FACSVerse or BD FACSCalibur (BD Biosciences). The following antibodies were used for flow cytometry: PE or APC-conjugated anti-FcεRI (MAR-1), AlexaFluor647- or FITC-conjugated anti-c-kit (2B8), biotinylated anti-mouse ST2 (RMST2-33) and APC-conjugated streptavidin. The 1–10 anti-SLC15A4 mAb was established by inoculating *Slc15a4*$^{-/-}$ mice with cells expressing SLC15A4, and the specificity was confirmed by flow cytometry (Supplementary Figure S4, available at *International Immunology* Online).

Separation of intracellular vesicles and cytosolic or nuclear fractions, and immunoblot analysis

BMMC intracellular vesicles were fractionated as previously described (6). Briefly, cells were suspended in extraction buffer (50 mM HEPES-OH pH 7.5, 78 mM KCl, 4 mM $MgCl_2$, 8.4 mM $CaCl_2$, 10 mM EGTA, 250 mM sucrose and 1× Halt Phosphatase Inhibitor) and homogenized by shear force using a 29-gauge needle with a syringe. The cell extracts were fractionated by 5–30% Opti-Prep (Sigma) gradient ultracentrifugation at 130 000 × *g* for 4 h. The fractionated vesicular proteins were separated by 4–20% SDS–PAGE and confirmed by immunoblotting. Cytosolic and nuclear fractions were separated by lysing BMMCs with extraction buffer for 10 min and centrifuging at 1000 × *g* for 5 min. The pellet was rinsed once with extraction buffer to remove leftover cytosol and was used as the nuclear fraction. The following antibodies were used for immunoblotting: anti-Stat3, anti-phospho-Stat3 (Tyr705), anti-phospho-Stat3 (Ser727), anti-Stat5, anti-phospho-Stat5 (Tyr694), anti-phospho-IκBα (Ser32/Ser36), anti-ERK1/2, anti-phospho-ERK1/2 (Thr202/Tyr204), anti-p38, anti-phospho-p38 (Thr180/Tyr182), anti-β-actin, anti-mTOR, anti-4EBP1, anti-phospho-4EBP1 (Thr37/46), anti-p70 S6 kinase, anti-phospho-p70 S6 kinase (Thr389), anti-S6, anti-phospho-S6 (Ser235/Ser236), anti-Rab7, anti-histone H3 (all from Cell Signaling Technology, MA, USA), anti-LAMP1 (1D4B), anti-Rab5, anti-Myc (9E10) (Santa Cruz Biotechnology, TX, USA), anti-IκBζ (Thermo Fisher) and anti-TFEB (Proteintech, IL, USA). For quantification of the band intensities, a LAS3000 (Fuji Photo Film, Tokyo, Japan) was used.

Retrovirus transduction

Slc15a4$^{-/-}$ mice were treated with 20 mg kg^{-1} 5-FU, and bone marrow cells were recovered 3 days later from the tibia and femur. Cells were cultured in RPMI 1640 medium supplemented with 10% fetal bovine serum, 2% streptomycin/penicillin, 10 ng ml^{-1} IL-3 (Peprotech), 10 ng ml^{-1} thrombopoietin (Wako Pure Chemical) and 100 ng ml^{-1} SCF (Peprotech) for 2 days. The retrovirus carrying WT or an E465K mutation of human SLC15A4 was introduced twice into the bone marrow cells, and 2 days after transduction, the cells were cultured for 8 weeks with RPMI 1640 medium supplemented with 10 ng ml^{-1} IL-3 and selected with puromycin (2 μg ml^{-1}). Myc-tagged

human TFEB-WT, -S142A or -4RA (R245A, R246A, R247A, R248A) was introduced into the RBL2H3 or P815 cells.

Immunofluorescence

Mouse BMMCs were fixed with PBS containing 4% paraformaldehyde (PFA) and 0.25% glutaraldehyde for 30 min at 4°C. After fixation, cells were permeabilized with 1× Perm Wash (BD Biosciences) and stained with anti-Histamine polyclonal antibody (Immunostar, WI, USA) in combination with anti-β-galactosidase (Abcam, UK) and anti-LAMP1 followed by staining with fluorochrome-conjugated secondary antibodies: AlexaFluor568–anti-rabbit Ig(H+L), AlexaFluor488–anti-chicken IgY or AlexaFluor647–anti-rat Ig(H+L), respectively. Mouse peritoneal mast cells were prepared from the peritoneal lavage of WT mice using 70% Percoll-assisted density-gradient centrifugation, and were fixed with 4% PFA in PBS for 30 min at 4°C. After fixation, cells were permeabilized with 1× Perm Wash (BD Biosciences) and stained with the 1–10 anti-SLC15A4 mAb in combination with anti-β-galactosidase, or anti-LAMP1 followed by staining with fluorochrome-conjugated secondary antibodies: AlexaFluor568–anti-mouse Ig(H+L), AlexaFluor488–anti-chicken IgY or AlexaFluor647–anti-rat Ig(H+L), respectively. For Rab7 staining, cells were stained with 1–10 anti-SLC15A4 mAb in combination with anti-Rab7 (Cell Signaling Technology) followed by anti-mouse IgG1–eFlour570 (eBioscience) and AlexaFluor647–anti-rabbit Ig(H+L). For EEA-1 staining, peritoneal mast cells were stained with AlexaFluor488-conjugated anti-EEA1 (MBL, Nagoya, Japan) and the 1–10 mAb followed by anti-mouse IgG1–eFlour570. Subcellular distribution was visualized using an FV1000 confocal microscope (Olympus, Tokyo, Japan).

Gene expression assays

RNA from BMMCs was purified with the RNeasy Mini Kit (Qiagen, Germany) or ISOGEN (Nippon Gene, Japan) and reverse-transcribed using a SuperScript III cDNA Synthesis Kit (Thermo Fisher). Quantitative RT–PCR was conducted with a StepOne Plus Real-Time PCR System (Thermo Fisher) with specific primers and probes for mouse *Tnf*, *Il6* or *Hprt* (Thermo Fisher). Gene expressions were normalized to *Hprt*. The expression of *Hdc*, mast-cell proteases, the genes involved in the serotonin synthesis or lysosome-associated genes was quantified with the THUNDERBIRD SYBR qPCR mix (Toyobo, Tokyo, Japan) on a StepOne Plus Real-Time PCR System. The primers used in this study are listed in Supplementary Table S1, available at *International Immunology* Online.

Statistics

The statistical significance of differences in the mean ± SD of various groups was calculated with Student's two-tailed *t*-test unless otherwise noted. *P*-values less than 0.05 were considered statistically significant.

Results

Increased histamine and serotonin synthesis and secretion in Slc15a4$^{-/-}$ mast cells

WT and SLC15A4-deficient (*Slc15a4*$^{-/-}$) mice did not differ in the frequency of c-kit^{+}FcεRIα^{+} cells in peritoneal exudate cells or of toluidine blue-positive mast cells in the ear skin (Supplementary Figure S1A and B, available at *International Immunology* Online). In addition, the IL-3- or SCF-dependent DNA replication of *Slc15a4*$^{-/-}$ BMMCs was comparable to that of WT BMMCs (Supplementary Figure S1C, available at *International Immunology* Online), and mast-cell granule proteases were expressed in *Slc15a4*$^{-/-}$ mast cells (Supplementary Figure S1D and E, available at *International Immunology* Online). These results indicated that SLC15A4 was not important for the commitment to a mast-cell lineage or in mast-cell survival and proliferation. We next examined whether SLC15A4 deficiency altered mast-cell functions, particularly those mediated by secretory granules. Histamine secretion in response to FcεRI cross-linking was elevated in *Slc15a4*$^{-/-}$ mast cells (Fig. 1A), probably due to an increase in total cellular histamine (Fig. 1A). These results were consistent with our previous report that histidine and its metabolite, histamine, are increased in LAMP1^{+} fractions in *Slc15a4*$^{-/-}$ B cells (6). Histidine decarboxylase, which catalyzes histamine synthesis from histidine, was also elevated in *Slc15a4*$^{-/-}$ mast cells (Fig. 1B). Serotonin secretion was also greatly enhanced in *Slc15a4*$^{-/-}$ mast cells in the presence of FcεRI-mediated stimulation (Fig. 1C), although the enzymes involved in serotonin synthesis were expressed at similar levels in *Slc15a4*$^{-/-}$ and WT BMMCs (Supplementary Figure S1F, available at *International Immunology* Online). Notably, the secretion of both histamine and serotonin in the absence of FcεRI-mediated stimulation was significantly increased in *Slc15a4*$^{-/-}$ mast cells (Fig. 1A and C), indicating that SLC15A4 is required for the homeostatic regulation of mast-cell secretory granules.

We next examined whether SLC15A4 is involved in mast-cell degranulation. FcεRI cross-linking induced the surface expression of LAMP1 glycoproteins in WT BMMCs because LAMP1^{+} secretory granules fused to the plasma membrane, as previously reported (36). In *Slc15a4*$^{-/-}$ BMMCs stimulated by FcεRI cross-linking, both the frequency of LAMP1-expressing cells and the mean fluorescence intensity of cell-surface LAMP1 staining increased (Fig. 1D). To quantify degranulation, we assayed the release of β-Hex, and found that it was increased in *Slc15a4*$^{-/-}$ BMMCs compared with WT BMMCs, both in the absence and the presence of FcεRI cross-linking (Fig. 1E). The amount of β-Hex protein did not differ significantly in whole-cell lysates of WT and *Slc15a4*$^{-/-}$ BMMCs (the enzymatic β-Hex activities in WT and *Slc15a4*$^{-/-}$ BMMC lysates were 156.8 ± 22.6 and 134.2 ± 4.29, respectively). These results indicated that SLC15A4 is involved in regulating the exocytosis of mast-cell granules. FcεRI expression and IgE binding to the BMMC surface were equivalent in *Slc15a4*$^{-/-}$ and WT mast cells (Supplementary Figure S1A, available at *International Immunology* Online; Fig. 1F and G). Immunohistochemical analyses demonstrated that the *Slc15a4*$^{-/-}$ BMMCs contained enlarged LAMP1^{+} but β-galactosidase (β-Gal)$^{-}$ granules that contained histamine (Fig. 1H). Collectively, these results indicated that SLC15A4 plays a pivotal role in controlling secretory-granule quality and limiting the degranulation process.

SLC15A4 loss differentially affected systemic and local anaphylaxis

We next investigated whether the loss of SLC15A4 affects mast-cell-mediated anaphylactic reactions *in vivo*. After

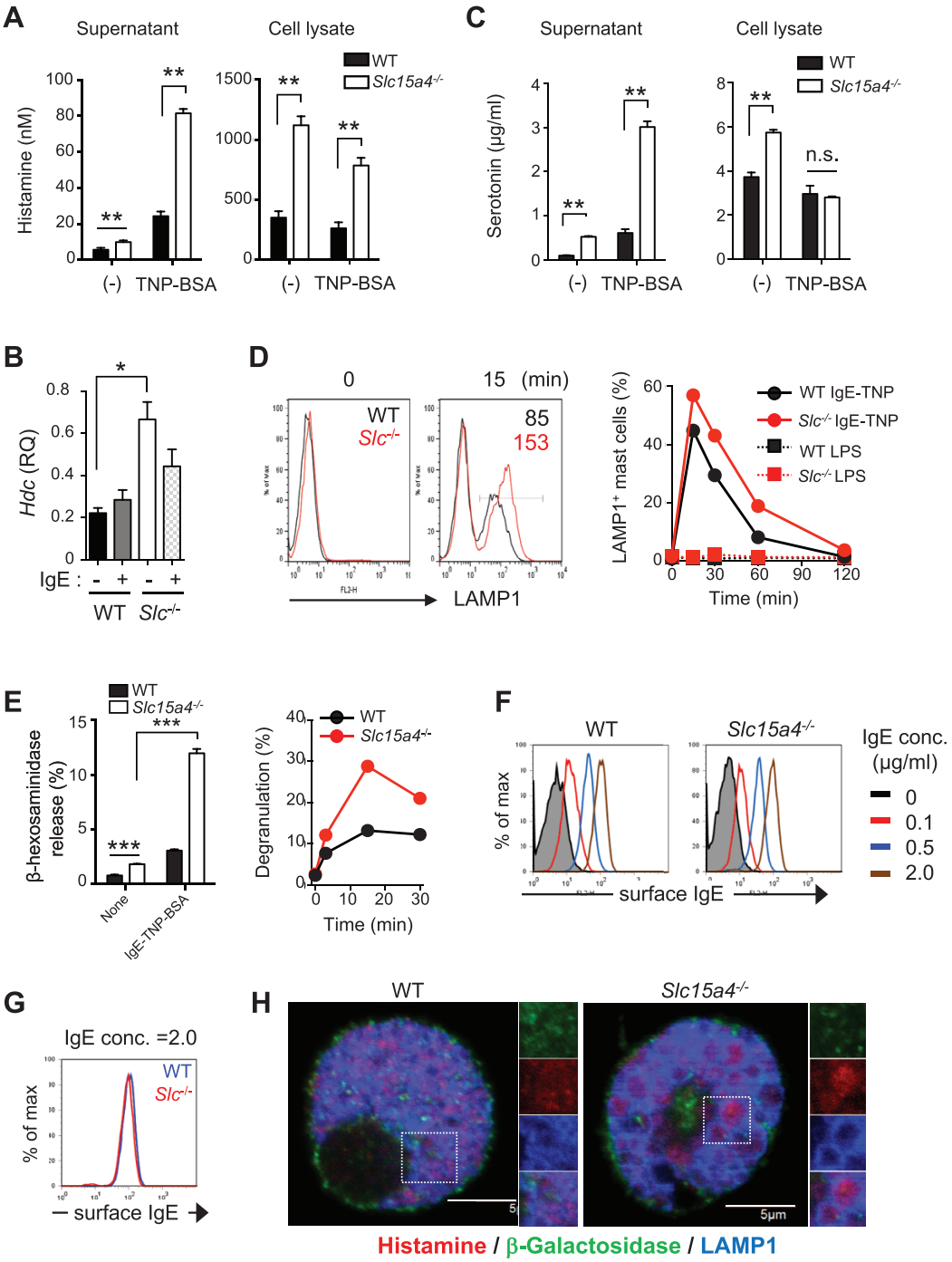

Fig. 1. SLC15A4 is required for the proper regulation of mast-cell effector functions. (A) Histamine levels in the culture supernatant or cell lysates of BMMCs from WT or *Slc15a4*$^{-/-}$ mice, determined by competitive EIA. Means and SD of three technical replicates are shown, and data are representative of three independent experiments. $^{**}P < 0.01$. (B) Histidine decarboxylase (*Hdc*) levels in WT and *Slc15a4*$^{-/-}$ BMMCs were determined by quantitative RT–PCR. Means and SD of three technical replicates are shown, and data are representative of three independent experiments. $^{*}P < 0.05$. (C) Serotonin in the culture supernatant or cell lysates of WT and *Slc15a4*$^{-/-}$ BMMCs upon IgE-mediated FcεRI ligation was quantified by competitive EIA. Means and SD of three technical replicates are shown, and data are representative of two independent experiments. $^{**}P < 0.01$. (D) Cell-surface LAMP1 was detected on WT and *Slc15a4*$^{-/-}$ BMMCs by flow cytometry. BMMCs were sensitized with anti-TNP IgE and stimulated by TNP_4-BSA. Histograms represent LAMP1 levels without stimulation or 15 min after stimulation, respectively (left). The proportion of LAMP1$^+$ cells was tracked during IgE-mediated degranulation (~120 min.) (right); LPS was used as a negative control. Results are representative of three independent experiments. (E) Degranulation of WT or *Slc15a4*$^{-/-}$ BMMCs was measured by β-Hex activity in the culture supernatant at 15 min (left), or over 30 min (right). $^{***}P < 0.001$. (F, G) IgE-binding capacity on the surface of WT or *Slc15a4*$^{-/-}$ BMMCs. The amount of bound IgE was measured by flow cytometry. Results are representative of three independent experiments. (H) Morphology of histamine-containing granules in BMMCs. The intracellular histamine in WT or *Slc15a4*$^{-/-}$ BMMCs was detected by anti-Histamine antibody and visualized on confocal microscopy. Results are representative of three independent experiments.

inducing passive systemic anaphylaxis with TNP-BSA and anti-TNP IgE antibodies, serum histamine levels were higher in *Slc15a4*$^{-/-}$ than in WT mice (Fig. 2A). The histamine concentrations in the steady-state sera were also higher in *Slc15a4*$^{-/-}$ than in WT mice (Fig. 2A), suggesting the steady-state secretion of histamine in *Slc15a4*$^{-/-}$ mice. Due to the increase of histamine in the steady state, the fold increase of serum histamine concentration in *Slc15a4*$^{-/-}$ mice was lower than in WT mice after FcεRI cross-linking (there were a 2.63- and 12.6-fold increase in *Slc15a4*$^{-/-}$ and WT mice, respectively). The transgenic complementation of *Slc15a4*$^{-/-}$ mice with SLC15A4 cDNA tended to decrease the serum histamine with or without antigenic stimulation (Fig. 2B), supporting SLC15A4's involvement in synthesizing and secreting histamine. Unexpectedly, the body temperature decreased similarly in *Slc15a4*$^{-/-}$ and WT mice during passive systemic anaphylaxis (Fig. 2C). This may be explained by a reduced response of *Slc15a4*$^{-/-}$ mice to histamine, possibly caused by histamine-receptor desensitization (37) due to increased levels of serum histamine in the steady state. This notion was supported by the finding that histamine-induced hypothermia was ameliorated in the *Slc15a4*$^{-/-}$ mice (Fig. 2D). Notably, FcεRI cross-linking induced cytokine secretion similarly in *Slc15a4*$^{-/-}$ and WT BMMCs (Fig. 2E; Supplementary Figure S2, available at *International Immunology* Online). These results suggested that in the context of FcεRI-mediated mast-cell activation, the early-phase secretion of preformed granules depended on SLC15A4, but *de novo*-synthesized cytokine secretion was less dependent.

SLC15A4 loss augmented IL-33-mediated inflammatory responses

IL-33 is released by damaged cells and elicits allergic inflammation by binding ST2 receptors on mast cells (31). We investigated whether SLC15A4 is also involved in IL-33-mediated mast-cell functions using an IL-33-triggered, antigen-dependent respiratory inflammation model (38) (Fig. 3A). *Slc15a4*$^{-/-}$ mice challenged with OVA in the presence of IL-33 showed an increase in monocyte numbers in the bronchoalveolar lavage fluid (BALF) compared with WT mice (Fig. 3B). The IL-33-induced TNFα and IL-6 secretion was augmented in *Slc15a4*$^{-/-}$ BMMCs (Fig. 3C), even though ST2L, a membrane-bound IL-33 receptor, was expressed similarly in WT and *Slc15a4*$^{-/-}$ BMMCs (Fig. 3D). IL-33-triggered IL-13 secretion did not differ significantly between WT and *Slc15a4*$^{-/-}$ mast cells (Fig. 3C). IL-33-triggered NFκB-pathway activation estimated by the phosphorylation and degradation of IκBα was unaffected by SLC15A4 loss (Fig. 3E). In contrast, ERK1/2 and STAT3 phosphorylation, particularly late-phase phosphorylation, were augmented in *Slc15a4*$^{-/-}$ mast cells in response to IL-33 stimulation (Fig. 3E). The augmentation of MyD88-mediated signaling was supported by the finding that the LPS-triggered secretion of TNFα and IL-6 also increased in *Slc15a4*$^{-/-}$ mast cells (Fig. 3F).

Our previous study using dendritic cells and B cells showed that the loss of SLC15A4 results in dysregulated vesicular pH, probably due to histidine accumulation, which is one of the causal factors of diminished TLR7/9 activation (6). In mast cells, however, there was no apparent dysregulation of vesicular pH (Supplementary Figure S3A and B, available at *International Immunology* Online). Although ST2 and SLC15A4 were partially colocalized in mast-cell vesicular compartments, disturbing the vesicular pH by Bafilomycin A1 treatment had little effect on IL-33-mediated cytokine production (Supplementary Figure S3C and D, available at *International Immunology* Online). These results suggested that IL-33-mediated signaling events in mast cells depend less on the vesicular pH than do the TLR7/9 signals in dendritic and B cells.

SLC15A4 distribution in mast cells

We next investigated which vesicles in mast cells contained SLC15A4. We established an anti-SLC15A4 mAb by inoculating SLC15A4 transfectants into *Slc15a4*$^{-/-}$ mice (Supplementary Figure S4A–C, available at *International Immunology* Online). The anti-SLC15A4 mAb (clone 1–10) specifically recognized both human and murine SLC15A4 but not the highly homologous family protein SLC15A3 (Supplementary Figure S4A–C, available at *International Immunology* Online). We then used this mAb to analyze the localization of endogenous SLC15A4. In the P815 murine mastocytoma cell line, some SLC15A4 proteins were distributed to intracellular vesicular compartments positive for LysoTracker and CD63 staining (Fig. 4A); these are considered to be lysosomes or LROs. Some SLC15A4 was distributed to LysoTracker-negative (non-acidic), CD63^{-} vesicular compartments (Fig. 4A). We further examined SLC15A4's distribution in peritoneal mast cells, and found that SLC15A4 localized to CD63^{+} vesicular compartments (Fig. 4B) and some SLC15A4 colocalized with or in the vicinity of LAMP1 (Fig. 4C). Although SLC15A4's localization appeared to be heterogeneous, hardly any localized to traditional β-Gal-containing lysosomes that perform degradation (Fig. 4C). SLC15A4's distribution was further investigated by organelle fractionation experiments, in which HA-tagged SLC15A4 was introduced into *Slc15a4*$^{-/-}$ BMMCs (since the 1–10 mAb was not applicable for western blot analyses). SLC15A4 proteins were highly enriched in the fractions containing LAMP1 and mTOR (fractions no. 4 and 5) but not in those containing β-Gal (Fig. 4D), consistent with our previous observations (6). Collectively, SLC15A4 localized to CD63-positive LROs, but not to degradative compartments in mast cells.

The mTOR–TFEB axis is involved in mast-cell cytokine production

We next investigated the mechanisms of SLC15A4-dependent mast-cell regulation. Since we previously demonstrated that SLC15A4 was required for mTORC1-dependent events in B cells and that SLC15A4 loss caused the dysregulation of mTORC1 association in B cells and BMMCs (6), we examined whether the loss of SLC15A4 disrupts mTORC1 signaling in mast cells. As expected, the mTORC1-dependent phosphorylation of 4E-BP1 and S6K was decreased in *Slc15a4*$^{-/-}$ compared with WT BMMCs (Fig. 5A). We next tried to clarify whether diminished mTORC1 activity could cause dysregulated mast-cell function. Torin 1, a specific mTORC1 inhibitor, decreased the phosphorylation of mTOR as well as its downstream target 4E-BP1 in mast cells (Fig. 5B). Treating WT

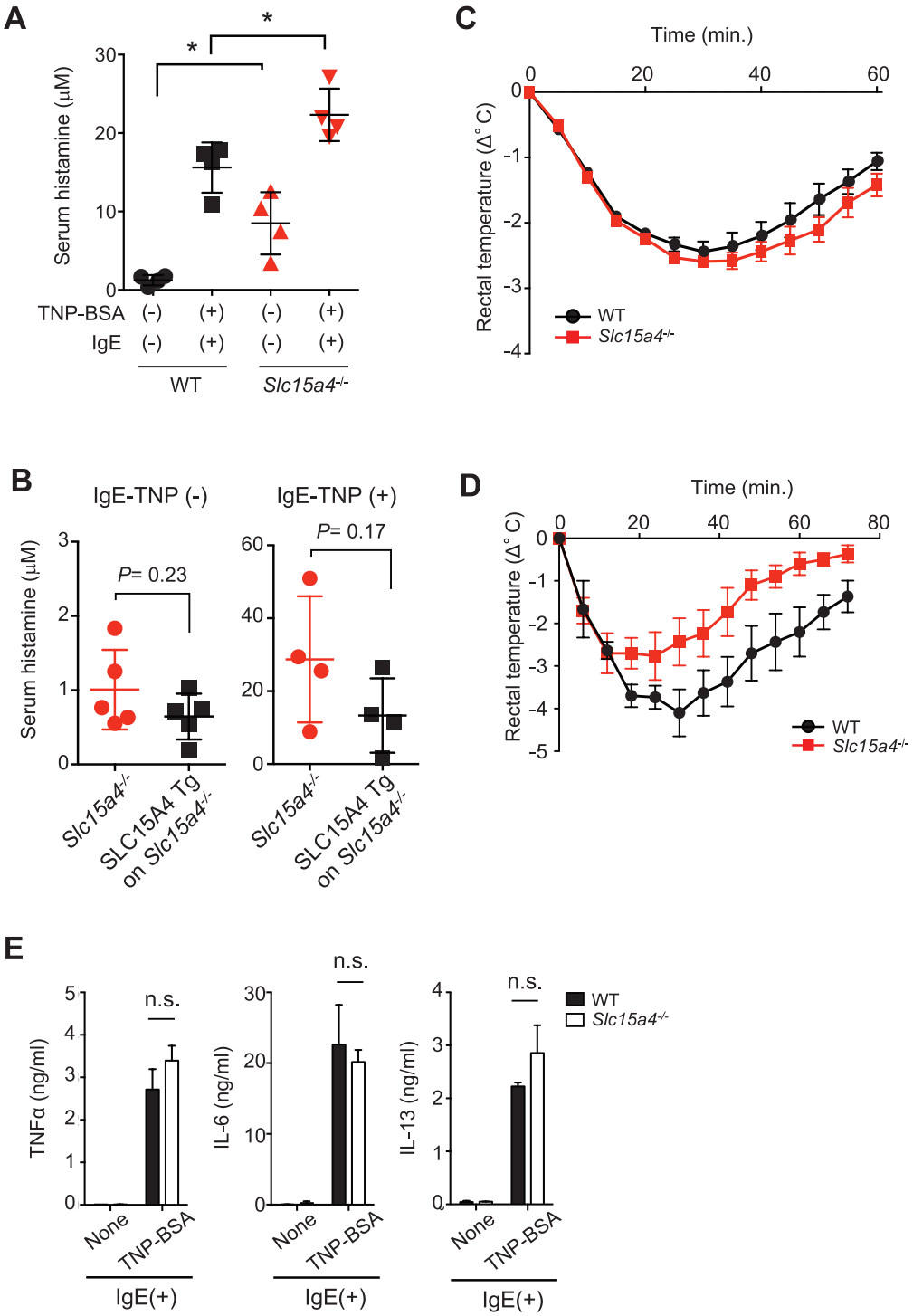

Fig. 2. SLC15A4 regulates histamine release *in vivo*. (A) Serum histamine levels during passive systemic anaphylaxis (PSA). WT (n = 4) or *Slc15a4*$^{-/-}$ (n = 4) mice were sensitized with anti-TNP IgE and challenged with TNP_4-BSA. Serum histamine levels 90 s after antigen challenge were determined by EIA. *P < 0.05. (B) Reversed histamine levels in mice expressing human SLC15A4. Serum histamine levels in the steady state or during PSA in transgenic *Slc15a4*$^{-/-}$ mice expressing human SLC15A4 and in control mice [n = 5 each for IgE-TNP (–), n = 4 each for IgE-TNP (+)] determined by histamine EIA. (C) Body-temperature changes during PSA. WT or *Slc15a4*$^{-/-}$ mice sensitized with anti-TNP IgE were challenged with TNP_4-BSA, and rectal temperature was monitored over 60 min (n = 5 for WT, n = 4 for *Slc15a4*$^{-/-}$). Results are representative of three independent experiments. (D) Body temperatures were monitored over 60 min during histamine-induced anaphylaxis in WT and *Slc15a4*$^{-/-}$ mice. Dots and error bars represent the mean and SE (n = 3 for both WT and *Slc15a4*$^{-/-}$, respectively). Results are representative of three independent experiments. (E) BMMC production of pro-inflammatory cytokines during IgE-mediated FcεRI ligation. WT or *Slc15a4*$^{-/-}$ BMMCs were stimulated for 6 h and cytokine levels in the culture supernatant were determined by ELISA (in technical triplicate). Results are representative of three independent experiments. n.s., not significant.

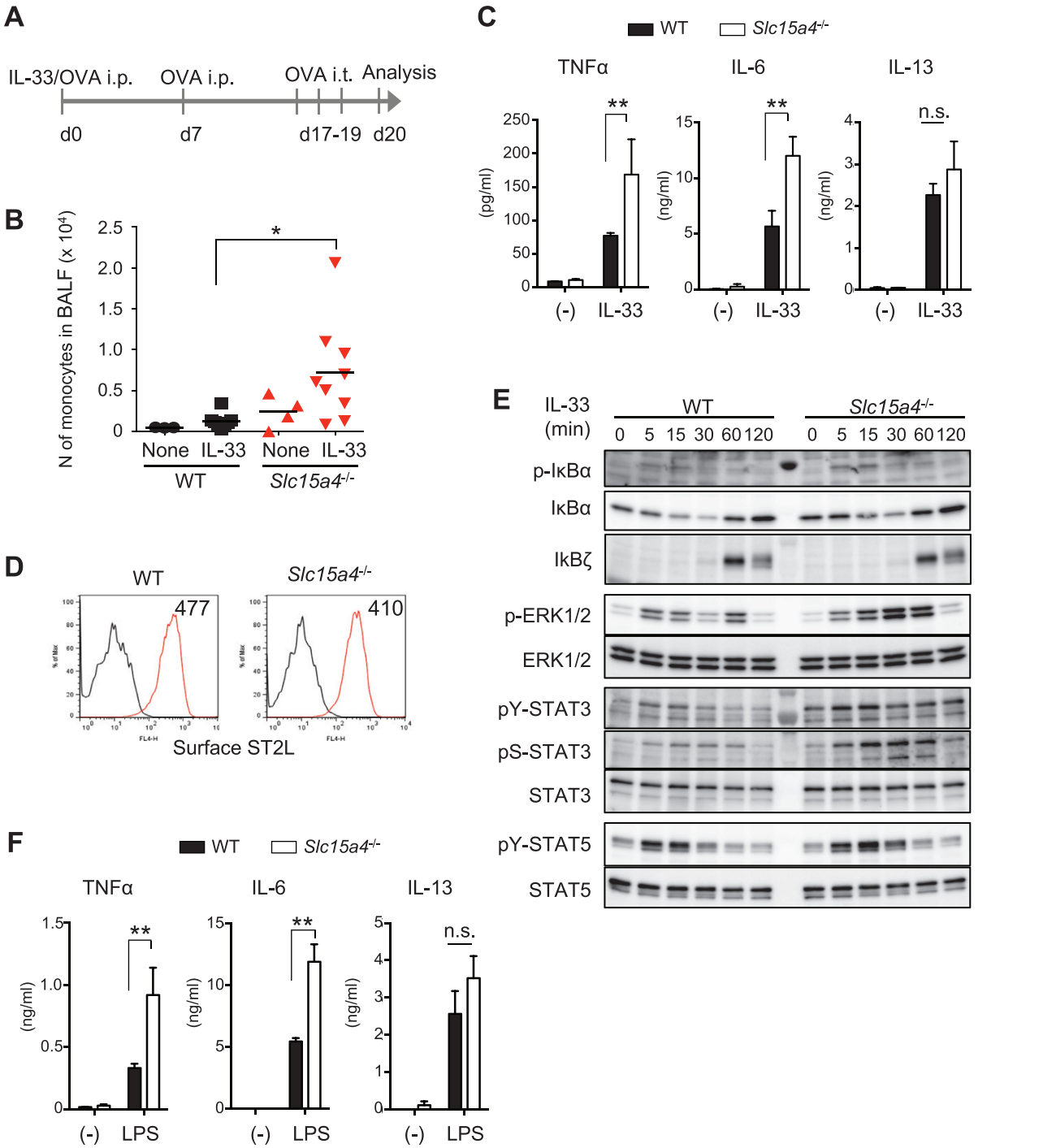

Fig. 3. SLC15A4-deficiency alters IL-33 signaling in mast cells. (A) Schematic of the IL-33-induced airway inflammation model. (B) Number of monocytes in the BALF before or after IL-33-induced inflammation in WT or *Slc15a4*$^{-/-}$ mice, analyzed by flow cytometry. Bars indicate the mean, and data are integrated from three independent experiments (n = 3 for WT none, n = 8 for WT IL-33, n = 4 for *Slc15a4*$^{-/-}$ none, n = 9 for *Slc15a4*$^{-/-}$ IL-33). *P < 0.05. (C) Cytokine production in response to IL-33 stimulation in BMMCs. TNFα, IL-6 and IL-13 levels in culture supernatants of WT or *Slc15a4*$^{-/-}$ BMMCs stimulated with recombinant IL-33 for 6 h measured by ELISA (in technical triplicate). Results are representative of four independent experiments. **P < 0.01; n.s., not significant. (D) Surface expression of the IL-33 receptor ST2L on BMMCs, analyzed by flow cytometry. (E) IL-33 signaling in WT or *Slc15a4*$^{-/-}$ BMMCs was analyzed by immunoblotting. WT or *Slc15a4*$^{-/-}$ BMMCs stimulated with recombinant IL-33 for the indicated periods were subjected to immunoblot analysis with the specific antibodies. (F) Cytokine production in WT or *Slc15a4*$^{-/-}$ BMMCs in response to LPS stimulation for 6 h; cytokine levels in the culture supernatant were measured by ELISA (in technical triplicate). For (D–F), results are representative of three independent experiments. **P < 0.01; n.s., not significant.

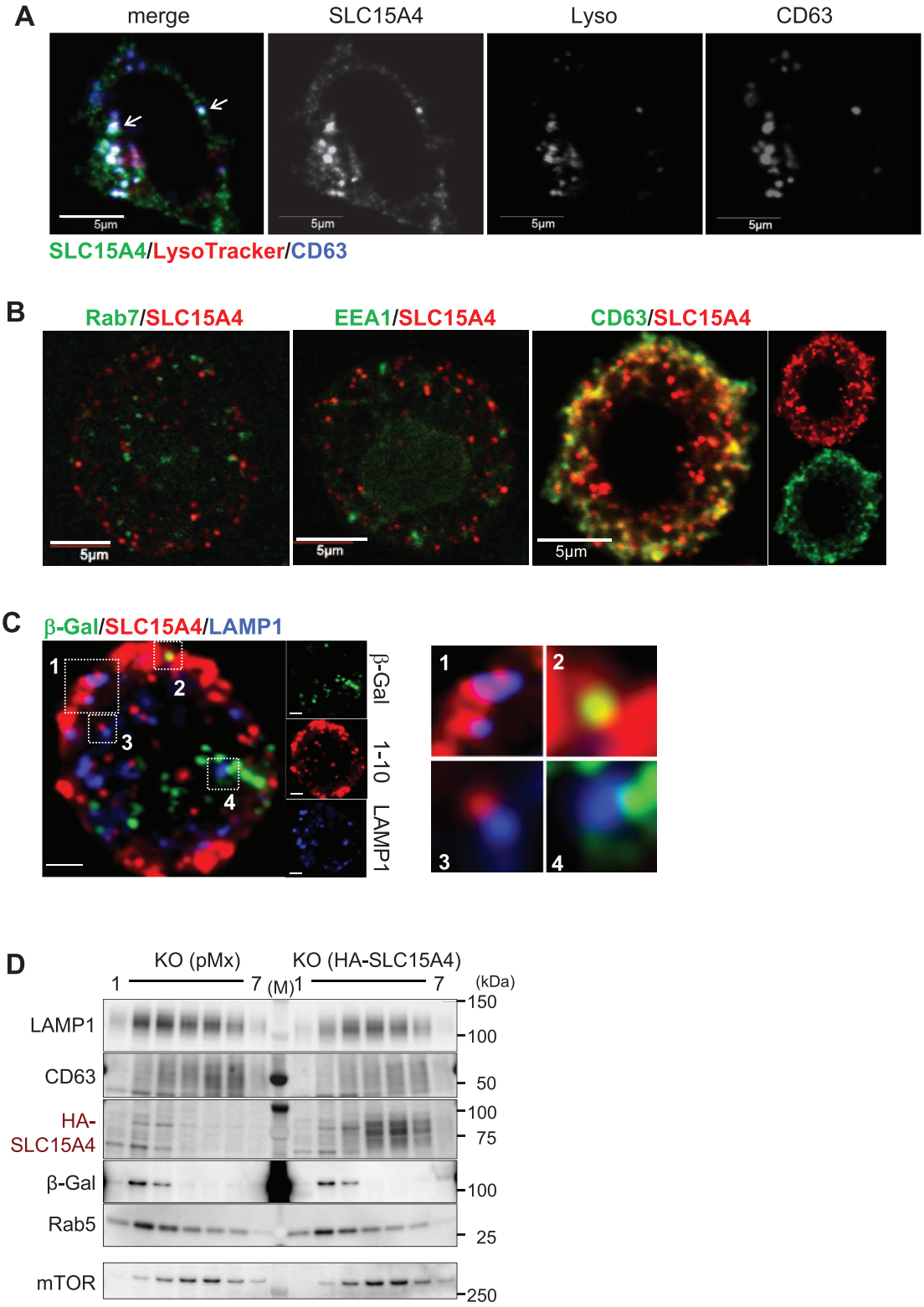

Fig. 4. SLC15A4's subcellular distribution in mast cells. (A) SLC15A4's subcellular distribution in a P815 mouse mastocytoma, visualized by confocal microscopy. LysoTracker or CD63 were used as the markers for the acidic compartment or the secretory granules, respectively. Results are representative of three independent experiments. (B, C) SLC15A4 subcellular distribution in WT peritoneal mast cells, visualized by confocal microscopy using LAMP1, Rab7, EEA1 and CD63 as markers for specific intracellular compartments. Results are representative of three independent experiments. (D) Distribution of SLC15A4^{+} vesicles in hematopoietic stem cell-derived *Slc15a4*$^{-/-}$ mast cells transduced with a control vector or HA-tagged human SLC15A4. Cell homogenate was fractionated, and markers for intracellular vesicles in each fraction were examined by western blotting; results are representative of three independent experiments.

mast cells with Torin 1 increased their IL-33-induced production of TNFα and IL-6 in a concentration-dependent fashion (Fig. 5C and D). Torin 1 treatment did not affect IL-13 production (Fig. 5E). These results suggested that the increased production of TNFα and IL-6 in *Slc15a4*$^{-/-}$ mast cells was at least partly due to the diminished activation of the mTORC1 pathway. Inhibiting mTORC1 by Torin 1 treatment had little effect on the FcεRI-mediated secretion of TNFα or IL-6 (Fig. 5F), consistent with our finding that FcεRI-mediated cytokine production was not affected by the loss of SLC15A4, as shown in Supplementary Figure S2, available at *International Immunology* Online.

SLC15A4 loss modified the CLEAR gene network through the mTORC1–TFEB signaling pathway

We further investigated how diminished mTORC1 activity affected mast-cell functions. We previously demonstrated that the loss of SLC15A4 caused the nuclear translocation of TFEB probably because of decreased TFEB phosphorylation mediated by mTORC1. Consistent with this scenario, TFEB's nuclear translocation was augmented in *Slc15a4*$^{-/-}$ BMMCs (Fig. 6A). Furthermore, the TFEB transcription was elevated in *Slc15a4*$^{-/-}$ BMMCs (Fig. 6B). This finding was consistent with the increased nuclear TFEB translocation in *Slc15a4*$^{-/-}$ BMMCs, since TFEB activity is autoregulated by a loop in which TFEB binds to its own promoter and induces its own transcription (14). We further found that among TFEB target genes, the transcription of a panel of genes involved in the CLEAR network was increased in *Slc15a4*$^{-/-}$ BMMCs (Fig. 6C). Electron microscopic analyses revealed anomalous vesicle formation in *Slc15a4*$^{-/-}$ mast cells (Fig. 6D), suggesting that SLC15A4 is involved in the biogenesis and/or homeostasis of LROs, including secretory granules.

We next sought to confirm that increased TFEB activity enhanced the transcription of CLEAR-network genes in *Slc15a4*$^{-/-}$ mast cells. Previous study demonstrated that elevated TFEB expression causes TFEB's nuclear translocation (15, 16). Here, we used the RBL-2H3 mast-cell line to establish stable transfectants with elevated TFEB levels (Fig. 6E). The transcription of CLEAR-network genes increased in transfectants expressing TFEB-WT or TFEB-S142A, in which the mTORC1 phosphorylation site at the serine 142 residue was replaced by alanine (Fig. 6F; Supplementary Figure S5, available at *International Immunology* Online), but it did not increase in transfectants expressing TFEB-4RA, which cannot translocate to the nucleus in mTOR-dependent manner (18) (Fig. 6F; Supplementary Figure S5, available at *International Immunology* Online). Taken together, these results indicated that SLC15A4 loss augmented TFEB's transcriptional activity, which altered LROs by affecting the CLEAR network.

TFEB's mTORC1-regulated nuclear translocation limits mast-cell secretory functions

We finally examined whether altering the mTORC1–TFEB axis could affect mast cells' secretory functions and responses to IL-33. Increased expression of TFEB-WT or TFEB-S142A but not of mock cDNA augmented lysosome exocytosis triggered by FcεRI cross-linking (Fig. 7A). Similar results were obtained in P815 transfectants (Fig. 7B). Notably, elevated TFEB also augmented the secretion of IL-6 both in the absence and presence of stimuli such as IL-33 or LPS (Fig. 7C and D), suggesting that elevated TFEB changes the basal set point of IL-6 secretion in mast cells. This augmentation did not occur in the P815 parental cell line or in mock transfectants. Elevated TFEB did not affect IL-13 secretion, probably because IL-13 was constitutively produced by P815 cells (Supplementary Figure S6, available at *International Immunology* Online). Furthermore, elevated TFEB did not affect FcεRI-mediated IL-6 secretion (Fig. 7E); again, this was consistent with our finding that IgE-dependent pro-inflammatory cytokine secretion did not differ between WT and *Slc15a4*$^{-/-}$ BMMCs, as shown in Fig. 2(E) and Supplementary Figure S2, available at *International Immunology* Online. Biochemical analyses of IL-33-mediated signaling events demonstrated that increases in TFEB enhanced ERK1/2 activation, particularly late-phase activation of ERK1/2 (Fig. 7F). This observation also supports the idea that increased TFEB expression plays a causal role in enhancing ERK1/2 activation in *Slc15a4*$^{-/-}$ mast cells. Taken together, these results strongly suggested that enhanced TFEB function, caused by diminished mTORC1 activity in the absence of SLC15A4, modified mast-cell-dependent inflammatory responses by altering secretory functions and IL-33-mediated signaling events.

Discussion

We here demonstrated that the amino-acid/oligopeptide transporter SLC15A4 is critical for secretory-granule homeostasis, which is necessary for mast-cell functions. Analyses of SLC15A4-deficient mast cells revealed that SLC15A4 limits the amino-acid-derived granule contents such as histamine and serotonin, leading to the novel concept that the amino-acid/oligopeptide flow from vesicular compartments to the cytosol is important for controlling mast-cell homeostasis and functions. The increase in histamine in secretory granules in *Slc15a4*$^{-/-}$ mast cells was not caused by inefficient degranulation, since both steady-state and FcεRI-mediated histamine release were elevated. We previously reported that SLC15A4 loss causes histidine and its metabolite, histamine, to accumulate in LAMP1^{+} compartments in B cells (6). Since histamine and serotonin are metabolites of histidine and tryptophan, respectively (39, 40), the accumulation of such amino acids in certain vesicular compartments might contribute to the increased storage of these mediators. However, the synthetic enzymes of these metabolites are cytoplasmic (41), and it is not clear whether the amino-acid accumulation is directly connected to the metabolite accumulation.

Notably, in *Slc15a4*$^{-/-}$ mast cells, the transcription of TFEB and a set of genes involved in the CLEAR network is augmented. Given that TFEB is a key regulator of lysosome biogenesis and adaptation (42), our results strongly suggest that TFEB's nuclear translocation, promoted by diminished mTORC1 activity, modulates LRO states via its transcriptional activity in *Slc15a4*$^{-/-}$ mast cells. The forced expression of WT or mutant TFEB confirmed that TFEB could activate the CLEAR network in mast cells and modulate mast-cell functions such as degranulation and response to IL-33. Although we did not investigate whether or how individual molecules involved in the CLEAR network connect functionally to

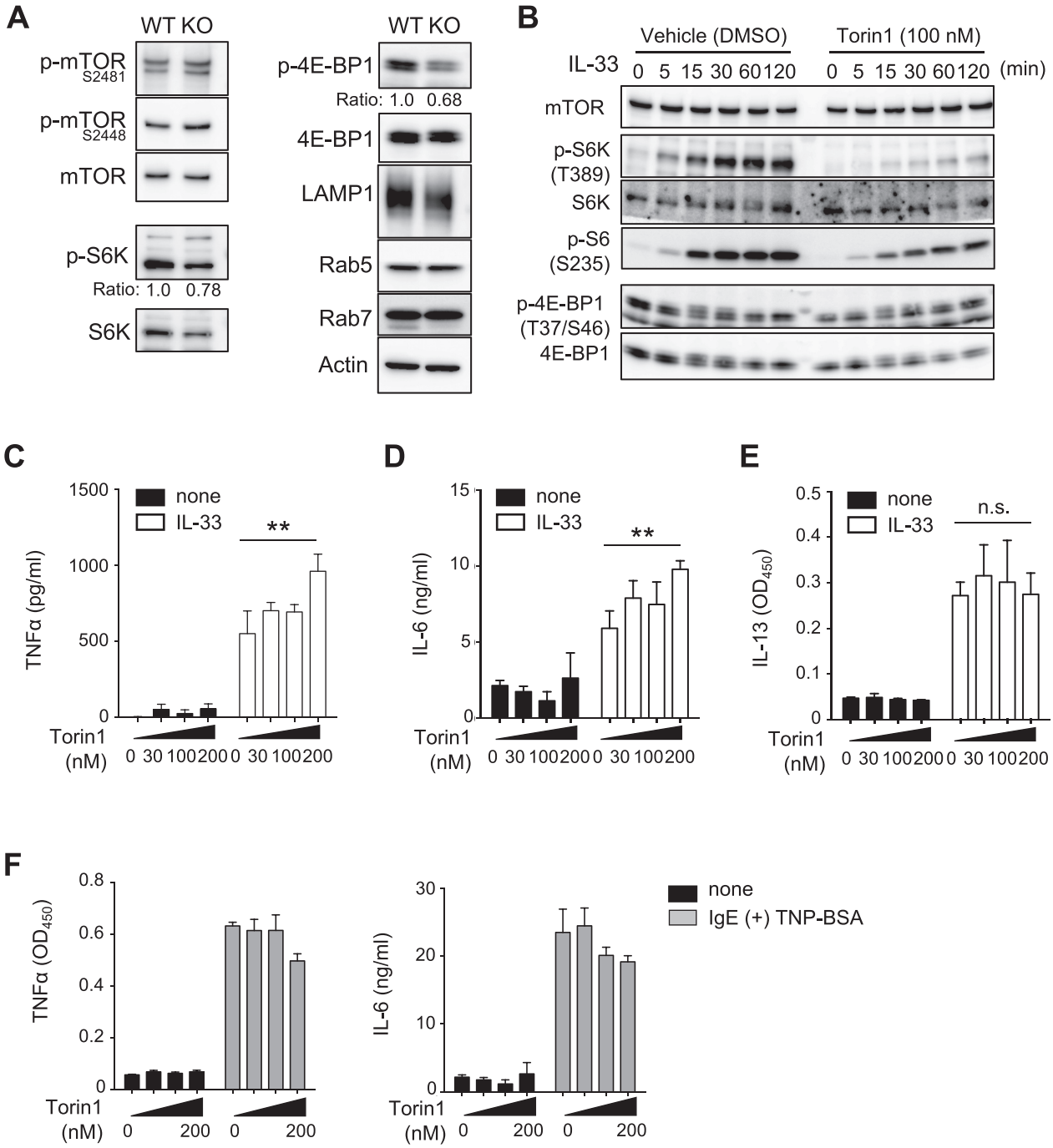

Fig. 5. SLC15A4 is required for mTOR activity in mast cells. (A) The mTOR pathway in BMMCs. Whole-cell extracts from WT or *Slc15a4*$^{-/-}$ BMMCs were analyzed by immunoblotting. Band intensities were measured by ImageJ software (NIH) and the relative phosphorylation ratio was indicated. (B–E) Pharmacological mTOR inhibition in IL-33 signaling in BMMCs. The mTOR signaling pathway during IL-33 stimulation (B) and levels of pro-inflammatory cytokines produced by WT BMMCs stimulated with recombinant IL-33 for 6 h in the presence of Torin 1 at the indicated concentrations (C–E). $^{**}P < 0.01$; n.s., not significant. (F) Effect of pharmacological mTOR inhibition in FcεRI-triggered cytokine production in BMMCs. The levels of pro-inflammatory cytokines produced by IgE-sensitized WT BMMCs stimulated with TNP_4-BSA for 6 h in the presence of Torin 1 at the indicated concentrations determined by ELISA (in triplicate). Results of both immunoblotting (A and B) and ELISA (C–F) and results are representative of three independent experiments.

mast-cell functions, augmented TFEB functions explained the enhanced granule exocytosis seen in *Slc15a4*$^{-/-}$ mast cells. A previous study reported that increased TFEB expression recruits lysosomes close to the plasma membrane, and this is required for lysosomal exocytosis (43). In fact, TFEB reverses pathologic lysosomal storage by promoting lysosomal exocytosis (43). Taken together with our finding that forced TFEB expression in mast-cell lines enhanced degranulation, the

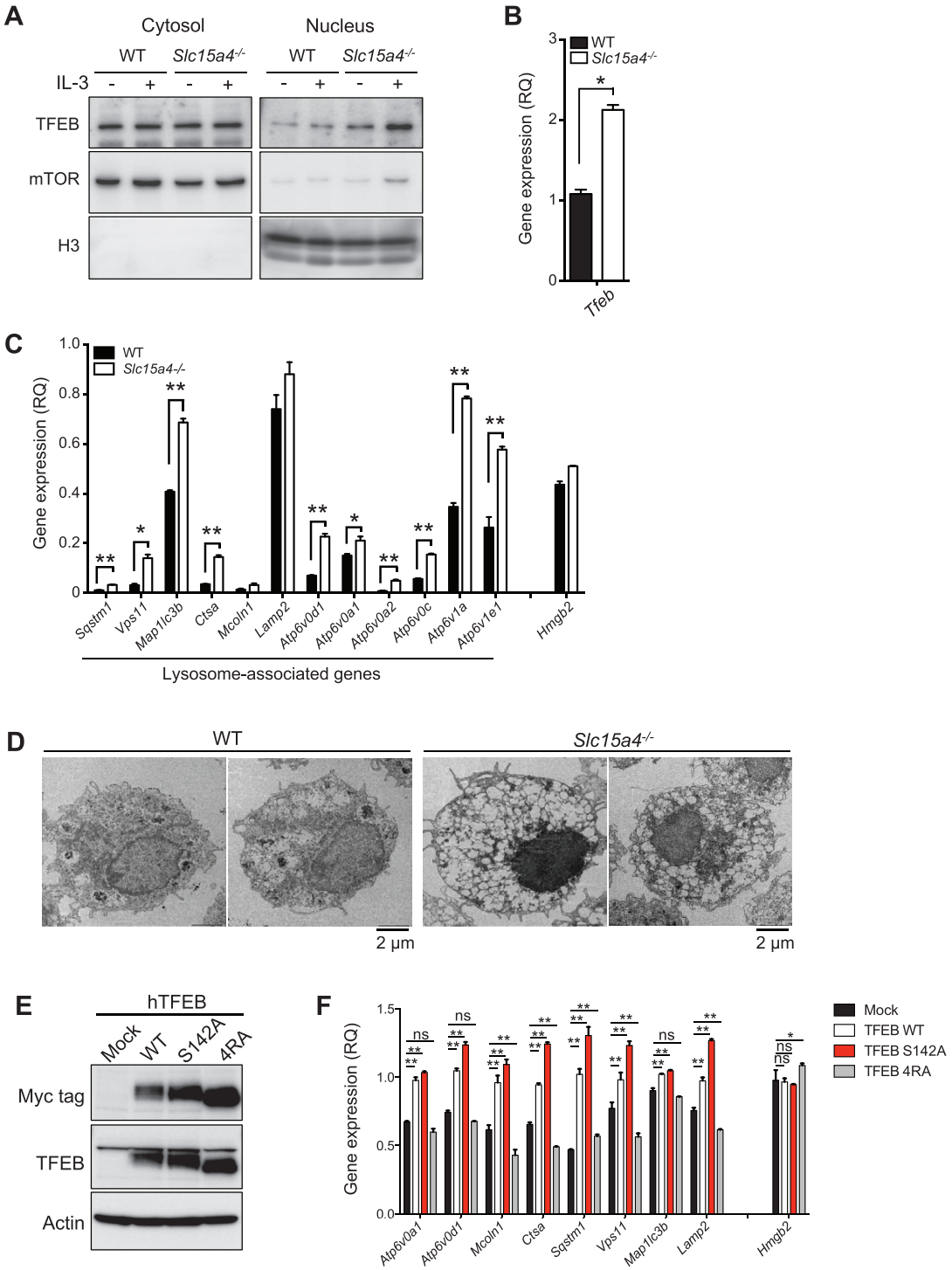

Fig. 6. SLC15A4 regulates the TFEB-mediated CLEAR network in mast cells. (A) The nuclear localization of the transcription factor TFEB in BMMCs. The cytosolic or nuclear fraction of WT or *Slc15a4*$^{-/-}$ BMMCs was analyzed by immunoblotting, and mTOR or histone H3 was used as cytosolic or nuclear reference, respectively. (B) TFEB expression levels in BMMCs; cDNA from WT or *Slc15a4*$^{-/-}$ BMMCs was assessed by quantitative RT-PCR. (C) Expression levels of lysosome-associated genes (the CLEAR network) in BMMCs. The cDNA from WT or *Slc15a4*$^{-/-}$ BMMCs was analyzed by quantitative RT-PCR. In (B) and (C), means and SD of three technical replicates are shown. Primer sets used in this experiment are listed in Supplementary Table S1, available at *International Immunology* Online. **P* < 0.05; ***P* < 0.01. (D) Morphology of intracellular vesicles in BMMCs. The superstructure of WT or *Slc15a4*$^{-/-}$ BMMCs was observed on transmission electron microscopy. (E) Protein expression of human TFEB mutants in RBL2H3 cells. RBL2H3 cells stably expressing Myc-tagged human TFEB WT or mutants were established, and their protein expression levels were analyzed by immunoblotting. (F) Expression levels of lysosome-associated genes in RBL2H3 cells expressing human TFEB mutants. The cDNA from RBL2H3 transfectants was analyzed by quantitative RT-PCR. **P* < 0.05; ***P* < 0.01; n.s., not significant, determined by Fisher's LSD. All data in Fig. 6 were representatives of more than three independent experiments.

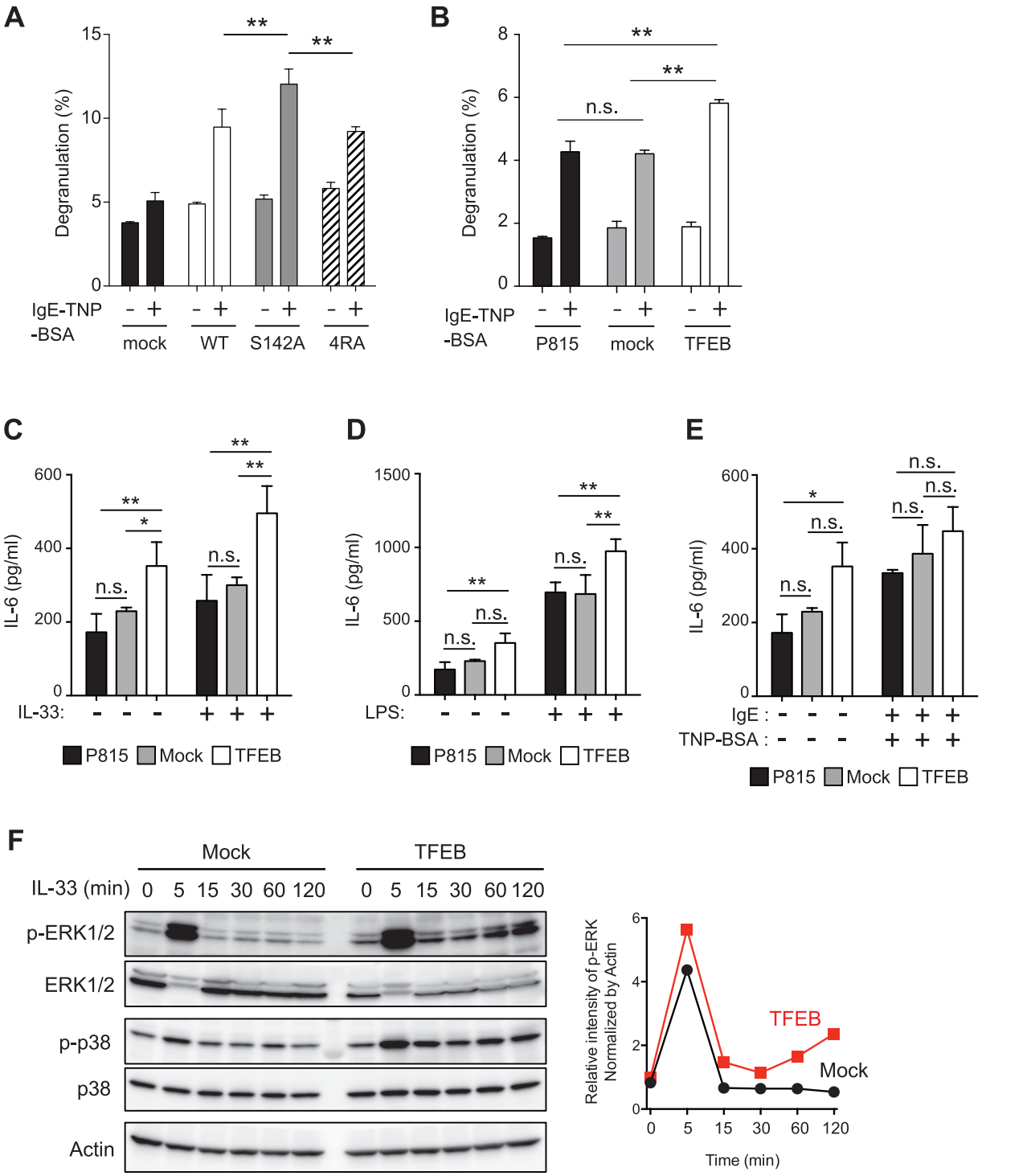

Fig. 7. Mast-cell effector functions depend on TFEB activity. (A, B) The degranulation of RBL2H3 transfectants expressing human TFEB mutants (A) or P815 transfectants expressing human TFEB-WT (B). RBL2H3 or P815 transfectants sensitized with anti-TNP IgE were stimulated with TNP_4-BSA for 30 min, and β-Hex activity in the supernatant or cell lysates was measured. Means and SD of three technical replicates are depicted. Results are representative of four independent experiments. (C–E) TFEB over-expression enhanced the response to IL-33 and LPS but not to FcεRI ligation. IL-6 levels in the culture supernatant of P815 transfectants stimulated with IL-33 (C), LPS (D) or IgE followed by TNP_4-BSA (E) for 24 h were determined by ELISA (in technical triplicate). $^*P < 0.05$; $^{**}P < 0.01$; n.s., not significant, determined by Tukey's test. Means and SD of three technical replicates are depicted. Results are representative of three independent experiments. (F) TFEB over-expression enhances IL-33 signaling. Whole-cell lysates from P815 mock-transfected cells (Mock) or from transfectants expressing human TFEB (TFEB) stimulated with recombinant IL-33 for the indicated periods were analyzed by immunoblotting. In the right side line plot, p-ERK1/2 band densities were measured by ImageJ and normalized against β-actin. Results are representative of three independent experiments.

augmented granule exocytosis in *Slc15a4*$^{-/-}$ mast cells might be a consequence of elevated TFEB expression and activity.

Slc15a4$^{-/-}$ mast cells produced high levels of pro-inflammatory cytokines in response to IL-33, indicating that SLC15A4 limits IL-33-mediated signaling events in mast cells. These high cytokine levels were also explained in part by dysregulated TFEB functions, since forced TFEB expression increased the IL-33-mediated IL-6 secretion. Based on our observations, it is plausible that TFEB facilitates the IL-33-dependent IL-6 production by altering ERK1/2 activity, since ERK1/2 activation in TFEB transfectants was elevated concomitantly with increased IL-6 secretion. However, the precise mechanisms by which increased TFEB expression enhances MAPK activation are unknown. Previous studies show that LAMTOR2/3 proteins form a scaffold for the ERK signaling complex at endosomes (44, 45), and that increased LAMTOR2/3 expression alone activates ERK (46). We observed that the amount of LAMTOR1 and LAMTOR2 proteins tended to increase in *Slc15a4*$^{-/-}$ mast cells (data not shown). Therefore, we hypothesize that the TFEB-mediated modulation of lysosomal biogenesis or adaptation enhances LAMTOR protein expression, increasing ERK's scaffolding potential. In addition, mTORC1's activity might directly contribute to IL-33's downstream signaling, since brief treatment with Torin 1 prior to IL-33 stimulation moderately enhanced the IL-33-dependent cytokine production.

Notably, our observations revealed an unexpected linkage between the dysregulation of the amino-acid/oligopeptide transporter SLC15A4 and the exacerbation of lung inflammation. Both mast cells and ILC2 cells are known to contribute to respiratory inflammation in the model we used (34, 38). Although the diminished response of *Slc15a4*$^{-/-}$ BMMCs to IL-33 supports the involvement of mast cells in IL-33-dependent inflammatory responses, the expression and significance of SLC15A4 in ILC2 cells should also be investigated. Moreover, since IL-33-dependent mast-cell functions are involved in the pathogenesis of various diseases such as food anaphylaxis (47), antiviral innate immunity (48) and respiratory inflammation induced by house dust mite or aspirin (49, 50), it might be important to investigate the significance of SLC15A4 in the pathogenesis of these diseases.

While a deeper mechanistic understanding of the augmented lung inflammation in *Slc15a4*$^{-/-}$ mice is still needed, our finding that the mTORC1–TFEB axis has a critical role in mast-cell functions opens the intriguing possibility that a sensing pathway exists in which nutrient signals modify mast-cell functions, since the mTORC1–TFEB signaling pathway is regulated according to nutritional conditions (12). Although this possibility requires further study, our findings offer an important insight into the close connection between nutritional sensing and allergic inflammation.

Although both FcεRI- and IL-33-mediated responses in mast cells require SLC15A4, the defects observed in FcεRI-mediated responses are an early event associated with the alteration of pre-synthesized granules, while those in IL-33-mediated cytokine production are a relatively late-phase event accompanied by *de novo* protein synthesis. As mentioned, both FcεRI-dependent degranulation and IL-33-mediated cytokine production are partly explained by elevated TFEB activity, and TFEB-dependent activation of the CLEAR network and the subsequent alteration or adaptation of lysosomes/LROs might occur prior to antigenic or inflammatory stimuli. Therefore, SLC15A4 appears to be necessary for the maturation or maintenance of mast cells, even though the differentiation of mast cells, as evaluated by surface markers such as c-kit and FcεRI, was not noticeably affected by SLC15A4 loss. Whether TFEB contributes to dysregulated histamine and serotonin storage in *Slc15a4*$^{-/-}$ mast cells is unclear. In the context of receptor downstream-signaling events after stimulation, the action schema of SLC15A4 in FcεRI downstream events seems to be distinct from that in IL-33 downstream events. FcεRI-mediated signaling events, including PLCγ and Akt phosphorylation and Ca^{2+} mobilization, were apparently unaffected by the loss of SLC15A4 (data not shown). Thus, neither SLC15A4 itself nor the mTORC1 pathway appears to be required for FcεRI-proximal signaling events; this conclusion is also supported by the observation that Torin 1 treatment did not affect FcεRI-mediated cytokine production. In IL-33-mediated signaling events, relatively early events such as IκBα phosphorylation or degradation progressed properly in the absence of SLC15A4. However, SLC15A4 loss affected later-phase signaling events such as ERK and STAT3 activation, which occur after IκBα phosphorylation and STAT5 phosphorylation. Therefore, it is conceivable that SLC15A4 deficiency affected the vesicular signaling compartment, where ST2L probably localized after being internalized. It remains to be clarified whether and how altered TFEB-mediated lysosome and/or LRO regulation is functionally attributed to the modification of vesicular signaling events.

Previous studies reported that rapamycin has no effect on FcεRI-triggered degranulation even though FcεRI cross-linking activates the mTORC1 pathway in human and mouse mast cells (51), suggesting that FcεRI-mediated degranulation does not require activation of the mTORC1 complex. This discrepancy with our results might be because a brief rapamycin treatment was insufficient to alter secretory-granule biogenesis or adaptation, which are accompanied by transcriptional changes. Therefore, we consider that the sustained reduction in mTORC1 activity seen in *Slc15a4*$^{-/-}$ mast cells (and also observed in transfectants after a sustained increase in TFEB) significantly accelerates degranulation by modulating the LRO state via the CLEAR network.

How SLC15A4's function is connected to mTORC1 regulation is still unclear. Since the mTORC1 activity is partly regulated by v-ATPase activity (52), and v-ATPase activity depends on vesicular pH (53), dysregulated granule acidity in *Slc15a4*$^{-/-}$ mast cells might decrease the mTORC1 activity (as we previously observed in B cells). However, we did not detect any dysregulation of the vesicular pH in *Slc15a4*$^{-/-}$ BMMCs, either in the presence or absence of stimuli. Furthermore, WT and *Slc15a4*$^{-/-}$ mast cells did not differ in the phosphorylation of GCN2 or its substrate, eIF2α (data not shown). These results may suggest that different mechanisms exist for sensing certain types of amino-acid or oligopeptide flow. It is important to clarify how a deficiency of a single amino-acid/oligopeptide transporter is linked to decreased mTORC1 activity, when mast cells possess multiple amino-acid transporters, including ABC-type transporters, for nutrient uptake.

Analyzing SLC15A4's intracellular localization is critical for advancing our understanding of SLC15A4's functions and the mechanisms that regulate signaling compartments in immune cells. We here used *Slc15a4*$^{-/-}$ mice to establish an anti-SLC15A4 mAb that was applicable for flow cytometry, immunohistochemistry and immunoprecipitation and made it possible to investigate the localization of endogenous SLC15A4. SLC15A4 was previously described as being lysosome-resident, a conclusion based partly on the observation that exogenously introduced, tagged SLC15A4 colocalizes with LAMP1 (6). However, our findings clarify that, at least in mast cells, SLC15A4 does not reside in typical β-Gal-containing lysosomes, which are clearance compartments, but instead localizes to CD63^{+} LROs or late endosomes. Since SLC15A4 was not distributed uniformly in these vesicular compartments, precise analyses of SLC15A4 distribution should be performed, from the perspective of vesicular trafficking.

In conclusion, our results indicated that the biogenesis and maintenance of secretory granules of mast cells is strictly dependent on SLC15A4. We revealed that SLC15A4 promotes the proper function of the mTORC1–TFEB axis in mast cells, and that TFEB dysregulation alters secretory-granule conditions, disturbing mast-cell secretory functions and the IL-33 signaling pathway. In addition, the results of an *in vivo* inflammatory model using *Slc15a4*$^{-/-}$ mice provide the intriguing possibility that mast cells' nutritional conditions are significant in T_h2 type immune responses. Although some aspects require further clarification, this study revealed a novel regulatory pathway for mast-cell functions.

Supplementary data

Supplementary data are available at *International Immunology* online.

Funding

This work was supported by the Funding Program for Next Generation World-Leading Researchers (Next Program) (for N.T.-S., LS134), grants-in-aid for Scientific Research from the Ministry of Education, Culture, Sports, Science, and Technology of Japan (for N.T.-S., 26293090; for T.K., 16K21654), Takeda Science Foundation (for T.K.) and a grant from the National Center for Global Health and Medicine (for N.T.-S., 23S001).

Acknowledgements

We thank Dr M. Tamura-Nakano (National Center for Global Health and Medicine) for technical assistance with the electron microscopy. We also thank Drs H. Karasuyama (Tokyo Medical and Dental University), L. A. Miglietta and G. E. Gray for critical reading of this manuscript, and N. Tanimura, H. Sorimachi and all department members for helpful discussions.

Conflicts of interest statement: The authors declared no conflicts of interest.

References

1 Yamashita, T., Shimada, S., Guo, W. *et al.* 1997. Cloning and functional expression of a brain peptide/histidine transporter. *J. Biol. Chem.* 272:10205.
2 Sasawatari, S., Okamura, T., Kasumi, E. *et al.* 2011. The solute carrier family 15A4 regulates TLR9 and NOD1 functions in the innate immune system and promotes colitis in mice. *Gastroenterology* 140:1513.
3 Blasius, A. L., Arnold, C. N., Georgel, P. *et al.* 2010. Slc15a4, AP-3, and Hermansky-Pudlak syndrome proteins are required for Toll-like receptor signaling in plasmacytoid dendritic cells. *Proc. Natl Acad. Sci. USA* 107:19973.
4 Lee, J., Tattoli, I., Wojtal, K. A., Vavricka, S. R., Philpott, D. J. and Girardin, S. E. 2009. pH-dependent internalization of muramyl peptides from early endosomes enables Nod1 and Nod2 signaling. *J. Biol. Chem.* 284:23818.
5 Blasius, A. L., Krebs, P., Sullivan, B. M., Oldstone, M. B. and Popkin, D. L. 2012. Slc15a4, a gene required for pDC sensing of TLR ligands, is required to control persistent viral infection. *PLoS Pathog.* 8:e1002915.
6 Kobayashi, T., Shimabukuro-Demoto, S., Yoshida-Sugitani, R. *et al.* 2014. The histidine transporter SLC15A4 coordinates mTOR-dependent inflammatory responses and pathogenic antibody production. *Immunity* 41:375.
7 Dosenovic, P., Ádori, M., Adams, W. C. *et al.* 2015. Slc15a4 function is required for intact class switch recombination to IgG2c in response to TLR9 stimulation. *Immunol. Cell Biol.* 93:136.
8 Marks, M. S., Heijnen, H. F. and Raposo, G. 2013. Lysosome-related organelles: unusual compartments become mainstream. *Curr. Opin. Cell Biol.* 25:495.
9 Appelqvist, H., Wäster, P., Kågedal, K. and Öllinger, K. 2013. The lysosome: from waste bag to potential therapeutic target. *J. Mol. Cell Biol.* 5:214.
10 Lim, C. Y. and Zoncu, R. 2016. The lysosome as a command-and-control center for cellular metabolism. *J. Cell Biol.* 214:653.
11 Hupalowska, A. and Miaczynska, M. 2012. The new faces of endocytosis in signaling. *Traffic* 13:9.
12 Settembre, C., Fraldi, A., Medina, D. L. and Ballabio, A. 2013. Signals from the lysosome: a control centre for cellular clearance and energy metabolism. *Nat. Rev. Mol. Cell Biol.* 14:283.
13 Dell'Angelica, E. C., Mullins, C., Caplan, S. and Bonifacino, J. S. 2000. Lysosome-related organelles. *FASEB J.* 14:1265.
14 Settembre, C., De Cegli, R., Mansueto, G. *et al.* 2013. TFEB controls cellular lipid metabolism through a starvation-induced autoregulatory loop. *Nat. Cell Biol.* 15:647.
15 Settembre, C., Di Malta, C., Polito, V. A. *et al.* 2011. TFEB links autophagy to lysosomal biogenesis. *Science* 332:1429.
16 Sardiello, M., Palmieri, M., di Ronza, A. *et al.* 2009. A gene network regulating lysosomal biogenesis and function. *Science* 325:473.
17 Settembre, C., Zoncu, R., Medina, D. L. *et al.* 2012. A lysosome-to-nucleus signalling mechanism senses and regulates the lysosome via mTOR and TFEB. *EMBO J.* 31:1095.
18 Roczniak-Ferguson, A., Petit, C. S., Froehlich, F. *et al.* 2012. The transcription factor TFEB links mTORC1 signaling to transcriptional control of lysosome homeostasis. *Sci. Signal.* 5:ra42.
19 Spampanato, C., Feeney, E., Li, L. *et al.* 2013. Transcription factor EB (TFEB) is a new therapeutic target for Pompe disease. *EMBO Mol. Med.* 5:691.
20 Wernersson, S. and Pejler, G. 2014. Mast cell secretory granules: armed for battle. *Nat. Rev. Immunol.* 14:478.
21 Moon, T. C., Befus, A. D. and Kulka, M. 2014. Mast cell mediators: their differential release and the secretory pathways involved. *Front. Immunol.* 5:569.
22 Henningsson, F., Hergeth, S., Cortelius, R., Abrink, M. and Pejler, G. 2006. A role for serglycin proteoglycan in granular retention and processing of mast cell secretory granule components. *FEBS J.* 273:4901.
23 Hallgren, J. and Gurish, M. F. 2014. Granule maturation in mast cells: histamine in control. *Eur. J. Immunol.* 44:33.
24 Krystel-Whittemore, M., Dileepan, K. N. and Wood, J. G. 2015. Mast cell: a multi-functional master cell. *Front. Immunol.* 6:620.
25 Galli, S. J. and Tsai, M. 2012. IgE and mast cells in allergic disease. *Nat. Med.* 18:693.
26 Sandig, H. and Bulfone-Paus, S. 2012. TLR signaling in mast cells: common and unique features. *Front. Immunol.* 3:185.
27 Sun, J., Sukhova, G. K., Wolters, P. J. *et al.* 2007. Mast cells promote atherosclerosis by releasing proinflammatory cytokines. *Nat. Med.* 13:719.
28 Miller, A. M. 2011. Role of IL-33 in inflammation and disease. *J. Inflamm. (Lond.)* 8:22.

29 Willart, M. A. and Hammad, H. 2010. Alarming dendritic cells for allergic sensitization. *Allergol. Int.* 59:95.
30 Theoharides, T. C., Alysandratos, K. D., Angelidou, A. *et al.* 2012. Mast cells and inflammation. *Biochim. Biophys. Acta* 1822:21.
31 Saluja, R., Khan, M., Church, M. K. and Maurer, M. 2015. The role of IL-33 and mast cells in allergy and inflammation. *Clin. Transl. Allergy* 5:33.
32 Stolarski, B., Kurowska-Stolarska, M., Kewin, P., Xu, D. and Liew, F. Y. 2010. IL-33 exacerbates eosinophil-mediated airway inflammation. *J. Immunol.* 185:3472.
33 Liew, F. Y., Pitman, N. I. and McInnes, I. B. 2010. Disease-associated functions of IL-33: the new kid in the IL-1 family. *Nat. Rev. Immunol.* 10:103.
34 Klein Wolterink, R. G. and Hendriks, R. W. 2013. Type 2 innate lymphocytes in allergic airway inflammation. *Curr. Allergy Asthma Rep.* 13:271.
35 Sayed, B. A., Christy, A., Quirion, M. R. and Brown, M. A. 2008. The master switch: the role of mast cells in autoimmunity and tolerance. *Annu. Rev. Immunol.* 26:705.
36 Betts, M. R., Brenchley, J. M., Price, D. A. *et al.* 2003. Sensitive and viable identification of antigen-specific CD8+ T cells by a flow cytometric assay for degranulation. *J. Immunol. Methods* 281:65.
37 Nakazawa, S., Sakanaka, M., Furuta, K. *et al.* 2014. Histamine synthesis is required for granule maturation in murine mast cells. *Eur. J. Immunol.* 44:204.
38 Heger, K., Fierens, K., Vahl, J. C. *et al.* 2014. A20-deficient mast cells exacerbate inflammatory responses *in vivo*. *PLoS Biol.* 12:e1001762.
39 Nowak, E. C., de Vries, V. C., Wasiuk, A. *et al.* 2012. Tryptophan hydroxylase-1 regulates immune tolerance and inflammation. *J. Exp. Med.* 209:2127.
40 Ohtsu, H., Tanaka, S., Terui, T. *et al.* 2001. Mice lacking histidine decarboxylase exhibit abnormal mast cells. *FEBS Lett.* 502:53.
41 Saxena, S. P., McNicol, A., Brandes, L. J., Becker, A. B. and Gerrard, J. M. 1989. Histamine formed in stimulated human platelets is cytoplasmic. *Biochem. Biophys. Res. Commun.* 164:164.
42 Settembre C. and Ballabio A. 2014. Lysosomal adaptation: how the lysosome responds to external cues. *Cold Spring Harb. Perspect. Biol.* 6:a016907.
43 Medina, D. L., Fraldi, A., Bouche, V. *et al.* 2011. Transcriptional activation of lysosomal exocytosis promotes cellular clearance. *Dev. Cell* 21:421.
44 Nada, S., Hondo, A., Kasai, A. *et al.* 2009. The novel lipid raft adaptor p18 controls endosome dynamics by anchoring the MEK-ERK pathway to late endosomes. *EMBO J.* 28:477.
45 Teis, D., Taub, N., Kurzbauer, R. *et al.* 2006. p14-MP1-MEK1 signaling regulates endosomal traffic and cellular proliferation during tissue homeostasis. *J. Cell Biol.* 175:861.
46 Schaeffer, H. J., Catling, A. D., Eblen, S. T., Collier, L. S., Krauss, A. and Weber, M. J. 1998. MP1: a MEK binding partner that enhances enzymatic activation of the MAP kinase cascade. *Science* 281:1668.
47 Galand, C., Leyva-Castillo, J. M., Yoon, J. *et al.* 2016. IL-33 promotes food anaphylaxis in epicutaneously sensitized mice by targeting mast cells. *J. Allergy Clin. Immunol.* 138:1356.
48 Aoki, R., Kawamura, T., Goshima, F. *et al.* 2016. The alarmin IL-33 derived from HSV-2-infected keratinocytes triggers mast cell-mediated antiviral innate immunity. *J. Invest. Dermatol.* 136:1290.
49 Zoltowska, A. M., Lei, Y., Fuchs, B., Rask, C., Adner, M. and Nilsson, G. P. 2016. The interleukin-33 receptor ST2 is important for the development of peripheral airway hyperresponsiveness and inflammation in a house dust mite mouse model of asthma. *Clin. Exp. Allergy* 46:479.
50 Liu, T., Kanaoka, Y., Barrett, N. A. *et al.* 2015. Aspirin-exacerbated respiratory disease involves a cysteinyl leukotriene-driven IL-33-mediated mast cell activation pathway. *J. Immunol.* 195:3537.
51 Kim, M. S., Kuehn, H. S., Metcalfe, D. D. and Gilfillan, A. M. 2008. Activation and function of the mTORC1 pathway in mast cells. *J. Immunol.* 180:4586.
52 Zoncu, R., Bar-Peled, L., Efeyan, A., Wang, S., Sancak, Y. and Sabatini, D. M. 2011. mTORC1 senses lysosomal amino acids through an inside-out mechanism that requires the vacuolar H(+)-ATPase. *Science* 334:678.
53 Sakai, H., Kawawaki, J., Moriura, Y., Mori, H., Morihata, H. and Kuno, M. 2006. pH dependence and inhibition by extracellular calcium of proton currents via plasmalemmal vacuolar-type H^+-ATPase in murine osteoclasts. *J. Physiol.* 576:417.